J|A|C|S
ARTICLES

Published on Web 11/19/2010

Water Is the Key to Nonclassical Nucleation of Amorphous Calcium Carbonate

Paolo Raiteri and Julian D. Gale*

Nanochemistry Research Institute, Department of Chemistry, Curtin University, P.O. Box U1987, Perth, WA 6845, Australia

Received September 21, 2010; E-mail: julian@ivec.org

Abstract: Calcium carbonate is a ubiquitous mineral that represents one of the most significant biominerals, a major contributor to carbon sequestration through geological deposits, and a technological hindrance as a result of scale formation. Amorphous calcium carbonate is intimately involved in the nucleation and growth of this material, yet much remains undiscovered regarding the atomic detail. Through dynamical simulation we demonstrate that nucleation of amorphous calcium carbonate follows a nonclassical pathway. This arises from the addition of ion pairs to clusters exhibiting a consistently exothermic free energy that persists with increasing particle size. Furthermore, the disruption of the surrounding water of solvation by the atomically rough surface reduces the barrier to growth to the order of ambient thermal energy, thereby allowing the amorphous phase to grow faster than crystalline polymorphs. Amorphous calcium carbonate nanoparticles are also found to exploit size-dependent water content to render itself more stable than the favored bulk phase, calcite, below a critical diameter of close to 4 nm.

Introduction

Calcium carbonate is one of the most significant naturally occurring minerals at the Earth's surface. It occurs widely as limestone deposits as well as coral reefs and represents a significant repository for carbon dioxide.[1,2] Organisms are capable of biomineralization of calcium carbonate to form skeletal and other materials.[3] Aside from the significance of this material in nature, the formation of scale from dissolved calcium ions and CO_2 in water makes the formation of this substance a technological problem, from the coating of vessels and pipe blockages to the fouling of desalination membranes.[4] Thus knowledge of the growth mechanisms of this substance is of fundamental importance to many fields.

Calcium carbonate ($CaCO_3$) occurs naturally in six different forms: three crystalline polymorphs, calcite, aragonite, and vaterite, in order of decreasing stability; two hydrate phases; and amorphous calcium carbonate (ACC). Of these, amorphous calcium carbonate is arguably the most important to growth processes since it can form the precursor to the crystallization of the other phases and plays a pivotal role in the process of biomineralization for this material.[3]

One of the reasons for the significance of ACC is that it has been argued that it allows calcium carbonate to circumvent conventional pathways for nucleation.[5] In classical nucleation theory, ions aggregate to form clusters that are initially unstable due to the entropic penalty for organization and the positive surface free energy of forming the crystal−solvent interface. As the particles increase in size, the cost of the surface energy is outweighed by the bulk lattice energy and so the system passes through a free energy maximum and then increases in stability with growing diameter. Competition between clusters possessing the structure of different polymorphs can occur through varying magnitudes of the free energy barrier leading to kinetic versus thermodynamic control.[6]

In the case of calcium carbonate, it has been proposed[5] that the system initially forms prenucleation nanoparticles of amorphous material that are stable, rather than metastable, though it has been suggested that this may be due to the presence of impurities.[7] Gebauer *et al*. observed the formation of two types of prenucleation nanoparticle with approximate sizes of 2 and 4 nm estimated from hydrodynamic measurements. Subsequently, Pouget *et al*.[8] confirmed the existence of such clusters using cryo-TEM, though while there was a distribution of sizes <4 nm, the majority of the particles were in the range of 0.6−1.1 nm. After several minutes, Pouget *et al*. observed the formation of ACC nanoparticles with a size of ∼30 nm, which they postulate form by aggregation of prenucleation clusters by Brownian motion. After further reaction, larger particles (>70 nm) appear, coinciding with the observation of polycrystalline material. The authors proposed that ACC is only (meta)stable to a size of ∼120 nm, while crystalline particles are stable above 70 nm, though the minimum size for an individual crystalline domain is unknown.

Larger nanoparticles of ACC can ultimately undergo a transition to a crystalline phase. The key to biomineralization is that the selection of the crystalline polymorph can be manipulated according to the environment of the ACC, especially the presence of organic macromolecules. Hence, an

(1) Kleypas, J. A.; Buddemeier, R. W.; Archer, D.; Gattuso, J. P.; Langdon, C.; Opdyke, B. N. *Science* **1999**, *284*, 118–120.
(2) Lackner, K. S. *Science* **2003**, *300*, 1677–1678.
(3) Weiner, S.; Sagi, I.; Addadi, L. *Science* **2005**, *309*, 1027–1028.
(4) Al-Anezi, K.; Hilal, N. *Sep. Purif. Rev.* **2006**, *35*, 223–247.
(5) Gebauer, D.; Volkel, A.; Colfen, H. *Science* **2008**, *322*, 1819–1822.
(6) Navrotsky, A. *Proc. Natl. Acad. Sci. U.S.A.* **2004**, *101*, 12096–12101.
(7) Meldrum, F. C.; Sear, R. P. *Science* **2008**, *322*, 1802–1803.
(8) Pouget, E. M.; Bomans, P. H. H.; Goos, J. A. C. M.; Frederik, P. M.; de With, G.; Sommerdijk, N. A. J. M. *Science* **2009**, *323*, 1455–1458.

organism can store preformed ACC and later select, as necessary, from forming calcite, aragonite, or vaterite.

Although ACC has been shown to be of critical importance to the growth of calcium carbonate, there remain significant gaps in our understanding of this form. Even to describe ACC as a single form of calcium carbonate is an oversimplification since it is known to occur as a variety of types, labeled transient, stable, unstable, and biogenic. Aside from the presence of impurities, such as magnesium[9] and phosphate that act to stabilize ACC, the main variable in the composition of ACC is the water content, which is believed to range from nominally dry calcium carbonate through to an approximate composition of $CaCO_3 \cdot H_2O$, though reports of at least 1.38 waters per formula unit exist.[10] Solid-state NMR indicates that the water is present predominately as a molecular entity and that there is little indication of the presence of bicarbonate species by proton exchange, though there may be some presence of OH^- due to the growth under basic conditions.[11] Other work has indicated that approximately half of the water molecules undergo hindered rotation with a time scale for reorientation of milliseconds.[10]

Structurally, there have been numerous attempts to characterize ACC. While techniques such as EXAFS can probe the local coordination environment of calcium, the advent of pair distribution function (PDF) analysis has provided more extended information on local atomic order. Comparison of the PDF patterns of ACC with those of other hydrous and anhydrous forms of calcium carbonate, as well data from ^{13}C NMR chemical shifts, shows that the structure of ACC does not resemble any known polymorph.[10] Very recently, Goodwin *et al*. have used PDF data to extract representative atomic coordinates for ACC through the use of Reverse Monte Carlo (RMC) simulations.[12] Their work suggests that the hydrous calcium carbonate forms a disordered Ca-rich framework with water forming chains within the pores. Whether this is a consequence of water being trapped during the agglomeration of prenucleation clusters or because of thermodynamic preference is unclear.

In the literature there has been considerable discussion regarding the instability of amorphous calcium carbonate as a function of conditions. The enthalpy of transition from ACC to calcite has been measured as between -4 and -15 ± 3 kJ/mol at the elevated temperatures (530−630 K) where water loss occurs.[13,14] Although there is a consensus that bulk ACC is unstable with respect to calcite, far less is known about the thermodynamics of this material during nucleation and the early stages of nanoparticle formation. To the best of our knowledge, the only quantitative thermodynamic information is that of Gebauer *et al.*, who show that the average free energy required to form an ion pair within a cluster varies between -18.5 and -17.3 kJ/mol, approximately, between pH values of 8.5 and 9.8, respectively.[5] This value is an average over several equilibria but critically indicates the stability of what are deemed prenucleation clusters. Given the experimental difficulties of accessing more detailed thermodynamic information for individual reaction steps, alternative methods of probing this critical stage in the growth process of the most important biomineral must be found. In the present work, we demonstrate that computer simulation can shed important light on this process, as it has done for other systems.[15−18]

While there have been extensive theoretical studies of crystalline calcium carbonate phases, including their bulk properties, surface structure, and morphology,[19] far less attention has been directed toward the amorphous material, especially with respect to the growth from aqueous solution. The most significant step to date is the work of Quigley and Rodger[20] who used metadynamics[21] (bias accelerated molecular dynamics) to explore the free energy surface of a 75 formula unit nanoparticle of calcium carbonate in water. Here they identified two distinct minima: one broad basin associated with an amorphous nanoparticle and a second, significantly less stable state characterized as a vaterite-like ordered structure. While representing a powerful advance, the practical problems of exploring the free energy landscape for a large number of nanoparticles of increasing dimensions means that the direct simulation of growth by applying an accelerating bias is currently impractical.

More recently, Tribello *et al*. have begun to consider the early stages of growth by considering the agglomeration of $CaCO_3$ ion pairs, as well as the direct simulation of the formation of ACC from a calcium carbonate solution.[22] Here they found that there was a negligible barrier to the formation of ACC clusters and so significant nucleation was observed on the time scale of several nanoseconds. Rather than being truly amorphous, it was found that their clusters are composed of misaligned domains of aragonite and vaterite. Unfortunately, it was later demonstrated[23] that the force field employed in this work fails to quantitatively describe the free energy differences between phases, as well as yielding an enthalpy of dissolution for calcite that leads to a significant underestimation in the solubility of this phase. Combined, these factors imply that nucleation will be far slower than observed in this study (and therefore will be inaccessible to direct simulation) and the observation of particular crystalline domains in ACC may not be accurate under the present conditions.

All previous computer simulations of amorphous calcium carbonate[20,22,24,25] have employed one of two different force fields[26,27] that have important failings in their description of

(9) Politi, Y.; Batchelor, D. R.; Zaslansky, P.; Chmelka, B. F.; Weaver, J. C.; Sagi, I.; Weiner, S.; Addadi, L. *Chem. Mater.* **2010**, *22*, 161–166.
(10) Michel, F. M.; MacDonald, J.; Feng, J.; Phillips, B. L.; Ehm, L.; Tarabrella, C.; Parise, J. B.; Reeder, R. J. *Chem. Mater.* **2008**, *20*, 4720–4728.
(11) Nebel, H.; Neumann, M.; Mayer, C.; Epple, M. *Inorg. Chem.* **2008**, *47*, 7874–7879.
(12) Goodwin, A. L.; Michel, F. M.; Phillips, B. L.; Keen, D. A.; Dove, M. T.; Reeder, R. J. *Chem. Mater.* **2010**, *22*, 3197–3205.
(13) Koga, N.; Nakagoe, Y. Z.; Tanaka, H. *Thermochim. Acta* **1998**, *318*, 239–244.
(14) Wolf, G.; Gunther, C. *J. Therm. Anal. Calorim.* **2001**, *65*, 687–698.
(15) Piana, S.; Reyhani, M.; Gale, J. D. *Nature* **2005**, *438*, 70–73.
(16) Piana, S.; Jones, F.; Gale, J. D. *J. Am. Chem. Soc.* **2006**, *128*, 13568–13574.
(17) Piana, S.; Jones, F.; Gale, J. D. *CrystEngComm* **2007**, *9*, 1187–1191.
(18) Page, A. J.; Sear, R. P. *J. Am. Chem. Soc.* **2009**, *131*, 17550–17551.
(19) de Leeuw, N. H.; Parker, S. C. *J. Phys. Chem. B* **1998**, *102*, 2914–2922.
(20) Quigley, D.; Rodger, P. M. *J. Chem. Phys.* **2008**, *128*, 221101.
(21) Laio, A.; Parrinello, M. *Proc. Natl. Acad. Sci. U.S.A.* **2002**, *99*, 12562–12566.
(22) Tribello, G. A.; Bruneval, F.; Liew, C.; Parrinello, M. *J. Phys. Chem. B* **2009**, *113*, 11680–11687.
(23) Raiteri, P.; Gale, J. D.; Quigley, D.; Rodger, P. M. *J. Phys. Chem. C* **2010**, *114*, 5997–6010.
(24) Quigley, D.; Rodger, P. M.; Freeman, C. L.; Harding, J. H.; Duffy, D. M. *J. Chem. Phys.* **2009**, *131*, 094703.
(25) Freeman, C. L.; Harding, J. H.; Quigley, D.; Rodger, P. M. *Angew. Chem., Int. Ed.* **2010**, *49*, 5135–5137.
(26) Freeman, C. L.; Harding, J. H.; Cooke, D. J.; Elliott, J. A.; Lardge, J. S.; Duffy, D. M. *J. Phys. Chem. C* **2007**, *111*, 11943–11951.
(27) Bruneval, F.; Donadio, D.; Parrinello, M. *J. Phys. Chem. B* **2007**, *111*, 12219–12227.

aqueous calcium carbonate systems; namely, they either incorrectly predict that aragonite is the most stable phase or conversely overstabilize calcite and thus cannot be used to describe competition between polymorphs reliably, while also failing to reproduce the experimental free energies of solvation of the calcium cation or carbonate anion correctly. This second failing leads to a significant underestimation of the solubility of calcium carbonate and qualitatively changes the association processes during growth. Most other literature force fields[28,29] share one or more of these limitations, while the overstabilization of the high-pressure calcite II structure is another possible pitfall of some models.[27,30] However, Raiteri *et al*.[23] have recently introduced a new force field that addresses all of the aforementioned issues, thus rendering the reliable simulation of calcium carbonate growth from aqueous solution possible.

In the present work we use computer simulation to explore the stability and growth thermodynamics of amorphous calcium carbonate nanoparticles over the range of sizes relevant to prenucleation (<∼4 nm). Importantly, we examine the size dependent hydration state of the nanoparticles and thereby provide a rationale for the existence of stable clusters as seen in the observations of Gebauer *et al*.[5] By comparing the thermodynamics of both ACC and crystalline nanoparticles of calcium carbonate as a function of size we are able to propose an explanation and thermodynamic model for the nonclassical growth of this material.

Methods

Force Field. Critical to the accuracy of any simulation is the quality of the force field. As already noted, we have recently created a new force field[23] for aqueous calcium carbonate systems that has been extensively validated against experimental thermodynamic data, including the free energy difference between calcite and aragonite, the free energy of solvation of the component ions, and the enthalpy of dissolution for calcite, as well as structural data and properties for relevant phases. This force field employs a rigid description of the carbonate anion and water (TIP4-Ew[31]). For the current work we have chosen to modify this model to include molecular flexibility. Although the use of rigid units allows a longer time step to be employed in molecular dynamics simulations, potentially making this type of model faster, in practice the restrictions created by the use of rigid units and the cost of the more complex algorithm required to propagate the configurations mean that a flexible model can be more efficient overall. Furthermore, it turns out that the thermodynamics of the vaterite polymorph are strongly dependent on the angular flexibility of the carbonate group. While both the calcite and aragonite structures constrain the carbonate anion to having a perfect 120° bond angle by symmetry, this is not the case in the disordered vaterite phase.

Starting from the parameters of Raiteri *et al*.,[23] we have refitted this model to include harmonic terms for bond, bond-angle, and out of plane distortion of the carbonate group. Indeed, it was possible to retain all the same intermolecular terms for calcium carbonate as per the rigid model, with only the addition of the intramolecular parameters that have been fitted against the vibrational modes of calcite.[32] All fitting to solid phases was performed with the GULP code[33,34] using the relaxed fitting algorithm.[35] With the change to a flexible carbonate, it was also appropriate to employ a different, flexible model for water. Here we have chosen to use the SPC/Fw model[36] whose properties have already been characterized and form the basis for a recent reactive MSEVB model[37] of proton transport. To compensate, the calcium− and carbonate−water interactions were slightly modified to ensure that the correct free energies of solvation were retained. Because the SPC/Fw model employs a short-range cutoff of 9 Å, the same value was chosen for the calcium carbonate interactions. While the SPC/Fw model includes a long-range correction for the truncation of the potential, for the calcium carbonate potentials a taper is applied over the final 3 Å to ensure that the energy and forces smoothly go to zero at the cutoff. The final force field parameters are reported in Table 1.

Table 1. Force Field Parameters for the Simulation of Aqueous Calcium Carbonate Systems with a Flexible Model[a]

Buckingham	Interaction	A (eV)	ρ (Å)	C (eVÅ^6)
Ca−O	Intermolecular	3161.63	0.27151	0.0
Ca−C	Intermolecular	120 000 000	0.12	0.0
O−O	Intermolecular	63 840.20	0.19891	27.899
O−O$_w$	Intermolecular	12 534.46	0.2020	12.090
O−H$_w$	Intermolecular	396.30	0.2170	0.0

Lennard−Jones	Interaction	ε (eV)	σ (Å)
Ca−O$_w$	Intermolecular	0.00095	3.35
O$_w$−O$_w$	Intermolecular	0.00674	3.16549

Harmonic	Interaction	k_2 (eV Å^{-2})	r_0 (Å)
C−O	Intramolecular	35.9	1.313
O$_w$−H$_w$	Intramolecular	45.93	1.012

Angle-bending	Interaction	k_θ (eV rad^{-2})	θ_0 (deg)
O−C−O	Intramolecular	12.0	120.0
H$_w$−O$_w$−H$_w$	Intramolecular	3.291	113.24

Out of plane	Interaction	$k_{2\text{-oop}}$ (eV Å^{-2})	$k_{4\text{-oop}}$ (eV Å^{-4})
C−O/O/O	Intramolecular	20.796	360.0

[a] Intermolecular parameters are as per Raiteri *et al*.[23] while the parameters for SPC/Fw water are from Wu *et al*.[36] All calcium and carbonate intermolecular terms are tapered to zero over the range of 6−9 Å. Here the symbol O refers to the oxygen of carbonate, while O$_w$ refers to that of water. Charges on atoms are as follows (in a.u.): Ca +2, C +1.123285, O −1.041095, O$_w$ −0.82, H$_w$ +0.41.

The results of the new flexible force field are essentially very similar to our previously published rigid model, except where noted. Hence, we report only selected results for the new model in Table 2. In particular, we see that the reproduction of the free energy difference between calcite and aragonite is retained. Because of the introduction of flexibility the entropic contribution is now non-negligible, though still underestimated with respect to experiment.[38] In the case of vaterite, the assessment of the free energy difference is more complex since the structure is generally considered to feature carbonate orientational disorder. There are two different structures proposed for this material. The first is an orthorhombic structure proposed on the basis of diffraction studies,[39] while the second one has been predicted to be lower in energy based on first

(28) Kerisit, S.; Parker, S. C. *J. Am. Chem. Soc.* **2004**, *126*, 10152–10161.
(29) Rohl, A. L.; Wright, K.; Gale, J. D. *Am. Mineral.* **2003**, *88*, 921–925.
(30) Archer, T. D.; Birse, S. E. A.; Dove, M. T.; Redfern, S. A. T.; Gale, J. D.; Cygan, R. T. *Phys. Chem. Miner.* **2003**, *30*, 416–424.
(31) Horn, H. W.; Swope, W. C.; Pitera, J. W.; Madura, J. D.; Dick, T. J.; Hura, G. L.; Head-Gordon, T. *J. Chem. Phys.* **2004**, *120*, 9665–9678.
(32) Prencipe, M.; Pascale, F.; Zicovich-Wilson, C. M.; Saunders, V. R.; Orlando, R.; Dovesi, R. *Phys. Chem. Miner.* **2004**, *31*, 559–564.
(33) Gale, J. D.; Rohl, A. L. *Mol. Simul.* **2003**, *29*, 291–341.
(34) Gale, J. D. *Z. Kristallogr.* **2005**, *220*, 552–554.
(35) Gale, J. D. *Philos. Mag. B* **1996**, *73*, 3–19.
(36) Wu, Y. J.; Tepper, H. L.; Voth, G. A. *J. Chem. Phys.* **2006**, *124*, 024503.
(37) Wu, Y. J.; Chen, H. N.; Wang, F.; Paesani, F.; Voth, G. A. *J. Phys. Chem. B* **2008**, *112*, 467–482.
(38) Wolf, G.; Lerchner, J.; Schmidt, H.; Gamsjager, H.; Konigsberger, E.; Schmidt, P. *J. Therm. Anal.* **1996**, *46*, 353–359.
(39) Meyer, H. J. *Angew. Chem., Int. Ed.* **1959**, *71*, 678–678.

Table 2. Comparison of Calculated versus Experimental Structure and Properties for Calcium Carbonate Phases, As Well As the Calcium Ion in Water, Based on the Flexible Carbonate Model Given in Table 1[a]

Quantity	Experiment	Calculated
ΔH (aragonite → calcite) (kJ/mol)[38]	+0.44	−0.27
ΔG (aragonite → calcite) (kJ/mol)[38]	−0.84	−0.84
ΔH (vaterite → calcite) (kJ/mol)[63]	−3.4	−5.4
ΔG (vaterite → calcite) (kJ/mol)[63]	−2.9	−3.1
ΔH (calcite dissolution) (kJ/mol)[41]	−12.5	−38.6
Calcite unit cell, *a* (Å)[64]	4.99	4.93
Calcite unit cell, *c* (Å)	17.06	17.26
Calcite bulk modulus (GPa)[65]	73.46	87.7
Aragonite unit cell, *a* (Å)[66]	4.96	4.99
Aragonite unit cell, *b* (Å)	7.97	8.03
Aragonite unit cell, *c* (Å)	5.74	5.63
Monohydrocalcite unit cell, *a* (Å)[67]	6.09	6.19
Monohydrocalcite unit cell, *c* (Å)	7.54	7.48
Aqueous solution: Ca−O (Å)[68]	2.43	2.40
Aqueous solution: Ca coord. no.[68]	7.3	7.2

[a] Thermodynamic and structural data are for 298.15 K.

principles calculations.[40] Here we calculate the free energy based on an ordered form of the orthorhombic structure, which the current model finds to be marginally more stable than the theoretical hexagonal model of Wang and Becker.[40] However, it is important to correct the lattice dynamical free energy differences for the configurational entropy of the 3-fold carbonate disorder in vaterite, which we include in the value in Table 2. Based on this, the new flexible force field largely corrects the error of approximately 9 kJ/mol in the overestimation of the relative free energy of vaterite given by the earlier rigid parametrization.

The rigid model fortuitously yielded exactly the experimental enthalpy of dissolution for calcite,[41] −12.5 kJ/mol, demonstrating that the model correctly balances the stability of the solid phases with that of the ions in solution unlike other models. Although the new flexible model gives a more exothermic value of −38.6 kJ/mol for this quantity, both values are equivalent within the statistical error bars (we note that the uncertainties in enthalpy differences are larger than those for free energies since they are computed indirectly from the free energy and entropy changes). For comparison, previous force fields for aqueous carbonate systems yielded dissolution enthalpies in excess of +100 kJ/mol leading to $CaCO_3$ being far less soluble than it should be.

Another respect in which the flexible force field is superior to the rigid one is in the description of the hydrated forms of calcium carbonate. Comparison of the structural parameters for monohydrocalcite ($CaCO_3 \cdot H_2O$) for the two models against experiment demonstrates that the flexible model represents a significant improvement in all cell lengths. For ikaite ($CaCO_3 \cdot 6H_2O$) the situation is less clear-cut, since the individual cell parameters get worse, but overall the volume is better. In the current context, the quality of description of monohydrocalcite is the most relevant consideration since this approximates the experimental composition of hydrous ACC.

Molecular Dynamics Simulations. All molecular dynamics simulations have been performed in the NPT ensemble, unless otherwise stated, using a Nosé−Hoover thermostat and the barostat of Melchionna *et al*.,[42] with relaxation times of 0.1 and 1.0 ps, respectively. A time step of 1 fs was employed, which was found to maintain stability in the conserved quantity. Run lengths typically involved at least 1 ns of equilibration followed by 2 ns of data collection. However, longer simulations were employed as required to ensure sufficient statistical convergence. The majority of the simulations were performed with the program LAMMPS,[43,44] except free energy perturbation calculations, which were carried out using DL_POLY.[45] The protocol for free energy perturbation calculations was as per our previous work,[23] except for the use of soft-core potentials during the Lennard−Jones perturbation phase, as proposed by Hess and van der Vegt.[46] Free energy profiles for the interaction of species as a function of distance were determined using umbrella sampling with the minimum Ca−C distance as a collective variable, as proposed by Tribello *et al*.[22] These calculations employed the PLUMED software plug-in.[47] Typically we used a window spacing of 0.4 Å with a force constant of 96.485 kJ/mol/Å^2, though additional windows were added as necessary to ensure proper sampling of the free energy surface.

Creation of Nanoparticles. Two broad categories of nanoparticles have been examined in the present study. First, crystalline calcite nanoparticles were created by assuming that the most stable basal $(10\bar{1}4)$ surface plane dominates the morphology, as is the case macroscopically. For the hexagonal crystal structure of calcite it is possible to generate morphologies where all terminations are of this surface, leading to a rhombohedral crystallite. Second, nanoparticles of amorphous calcium carbonate were created with varying degrees of water content. Since the underlying structure and morphological details are unclear for this material we describe the procedure by which the particles are created in detail below.

To create an amorphous calcium carbonate particle we start by taking crystallites of ordered calcite *in vacuo* and annealing them at 3000 K until no residual structural order remains, as indicated by examination of the radial distribution function (RDF). We note that this temperature is not intended to be physical; its purpose is purely to accelerate the amorphization of the particle. Furthermore, the use of a molecular mechanics representation for the carbonate ion implies that decomposition will not occur, as it would in reality. Having created an amorphous particle, this is inserted into a cubic simulation cell containing up to 20 000 molecules of water with no prior creation of a cavity in the medium. Water molecules must then be removed based on the degree of overlap with the calcium carbonate atoms. For the $(10\bar{1}4)$ calcite−water interface, the first peak in the radial distribution function occurs at approximately 2 Å above the surface, corresponding to a Ca−O distance of 2.4 Å. Any water molecule at a greater distance from $CaCO_3$ than this value is therefore at an acceptable initial position and can remain. By successively excluding water molecules with shorter contact distances, we created amorphous nanoparticles with 5 different degrees of hydration, spanning anhydrous ACC through to a water content of just over 3 molecules per formula unit, for further examination. For smaller clusters, below 90 formula units, higher degrees of hydration are found, but at this size the uncertainty in the quantification of the water content is high due to the rough nature of the surface.

Having created initial configurations for the nanoparticles in water, the systems are equilibrated until the potential energy of the system reaches a plateau, thereby indicating that the particle is sampling a stable range of configurations on the nanosecond time scale. One of the most important questions to be considered here is whether the structures of the amorphous nanoparticles found are the relevant ones or not? Given the limited time scales of molecular dynamics simulations there is always the possibility that a strongly activated process will be missed. We have addressed this issue in a number of ways. First, different initial morphologies of the calcite nanoparticles have been used for amorphization in which surfaces other than the $(10\bar{1}4)$ face are expressed for the same size. This is

(40) Wang, J. W.; Becker, U. *Am. Mineral.* **2009**, *94*, 380–386.
(41) *Handbook of Chemistry and Physics*, 62nd ed.; CRC Press: Boca Raton, FL, 1981.
(42) Melchionna, S.; Ciccotti, G.; Holian, B. L. *Mol. Phys.* **1993**, *78*, 533–544.
(43) Plimpton, S. *J. Comput. Phys.* **1995**, *117*, 1–19.
(44) http://www.lampps.sandia.gov/.
(45) Smith, W.; Forester, T. R. *J. Mol. Graphics* **1996**, *14*, 136–141.
(46) Hess, B.; van der Vegt, N. F. A. *J. Phys. Chem. B* **2006**, *110*, 17616–17626.
(47) Bonomi, M.; Branduardi, D.; Bussi, G.; Camilloni, C.; Provasi, D.; Raiteri, P.; Donadio, D.; Marinelli, F.; Pietrucci, F.; Broglia, R. A.; Parrinello, M. *Comput. Phys. Commun.* **2009**, *180*, 1961–1972.

found to lead to no significant difference in the final results. Second, for the ACC clusters in water, the simulations were repeated with different initial random velocities to ensure that the final ensemble averages were consistent, as they indeed were. Third, the generation of different sized nanoparticles was performed independently. If the system had a tendency to become trapped in high energy minima then one would not expect to see systematic trends across particle sizes. As we will demonstrate later, systematic behavior is observed. Fourthly, as will also be shown below, the structural characteristics also agree well with those observed experimentally. Finally, while it would be expected that crystalline nanoparticles, such as those of calcite, will exhibit a large number of minima with barriers too high to overcome on the nanosecond time scale, and therefore the initial choice of morphology is critical, the amorphous material is relatively soft and can explore states more readily. Indeed, we observe that the ACC nanoparticles fluctuate slightly in shape on the time scale of the simulation, suggesting that it is unlikely that they would be trapped in an incorrect morphological state. While the use of accelerated dynamical methods, such as metadynamics, could prove valuable to search the configuration space in future, given a suitable set of collective variables, it appears very likely that the ACC nanoparticles are close to their ground state already.

A final issue that should be considered is whether it is appropriate to assume that ACC consists of calcium cations, carbonate anions, and water only. For example, at neutral pH the bicarbonate ion is the dominant species in solution, rather than carbonate.[48] However, ACC is generally synthesized under basic conditions driving this equilibrium toward carbonate. Furthermore, evidence from solid-state NMR indicates that the water is present predominately as a molecular entity and that there is little indication of the presence of bicarbonate species within ACC.[11] Therefore, although we do not explicitly consider pH in the present simulations, the basic conditions are implicit through the use of carbonate, whose dominant presence is supported by experiment.

Results and Discussion

Calcium carbonate clusters and nanoparticles have been generated for a range of sizes spanning 18 to 864 formula units of $CaCO_3$, according to the methodology previously described. Representative structures for the largest nanoparticles of calcite and amorphous calcium carbonate are illustrated in Figure 1. For the largest ACC nanoparticle considered, this corresponds to an approximate diameter of 5.5 nm, though we note that the boundary of such amorphous hydrated particles is not sharply defined due to the rough and fluctuating nature of the surface. Here the term "rough" is used to indicate the fact that the surface is uneven, of variable structure, including radial height, aperiodic, and therefore totally distinct from the situation found for a well-defined crystallographic plane. In Figure 2, the radial density distribution of calcium and water (as given by the position of oxygen) is presented for the largest 864 formula unit nanoparticle to illustrate the nature of the interface. The two extremes of hydration are shown: anhydrous ACC and a material with just over 3 water molecules per formula unit. For both particles, the decay of calcium ion density from that in the nanoparticle to solution occurs over a distance of approximately 5 Å. The apparent decay with radius is a consequence of averaging over the angular orientation; in reality the cutoff is sharper in any given direction, but the particle is not of uniform radius around the surface. As the calcium ion density decays, there is a corresponding increase in the water density beginning at the same radius. However, the radial density of water only reaches the limit of bulk aqueous solution after the distance is closer to 10 Å from the point at which the interface begins. This is a result of the structure of the water beyond the surface of the nanoparticle that leads to a slightly enhanced density at the radius where the calcium ion concentration effectively reaches zero. While the interface between the basal plane of calcite and aqueous solution has two strongly oriented water layers,[23,49] and arguably a third weakly structured layer, the combination of a rough surface and an underlying amorphous structure leads to no sharp peaks in the radial distribution function at the surface of ACC. The lack of a strongly structured hydration shell can be seen in Figure 3 where a 2-D cross section is taken through the water density surrounding the largest nanoparticle considered.

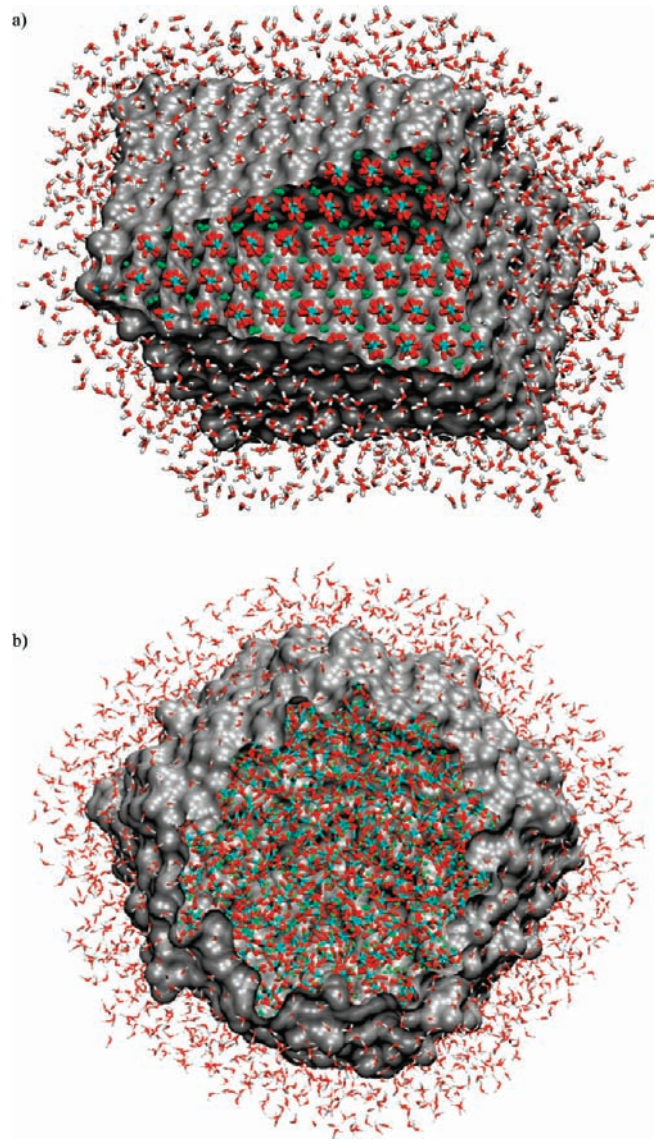

Figure 1. Illustration of two solvated nanoparticles of (a) calcite and (b) amorphous calcium carbonate. Both nanoparticles contain 864 formula units of $CaCO_3$, and the ACC is shown for the anhydrous material. Here calcium, carbon, oxygen, and hydrogen are colored green, blue, red, and white, respectively. Only the first few solvation shells are shown for clarity. To emphasize the shape of the nanoparticle, the van der Waals surface has been shown in gray, with part of the surface removed to allow viewing of the inner nanoparticle structure.

(48) Plummer, L. N.; Busenberg, E. *Geochim. Cosmochim. Acta* **1982**, *46*, 1011–1040.

(49) Geissbuhler, P.; Fenter, P.; DiMasi, E.; Srajer, G.; Sorensen, L. B.; Sturchio, N. C. *Surf. Sci.* **2004**, *573*, 191–203.

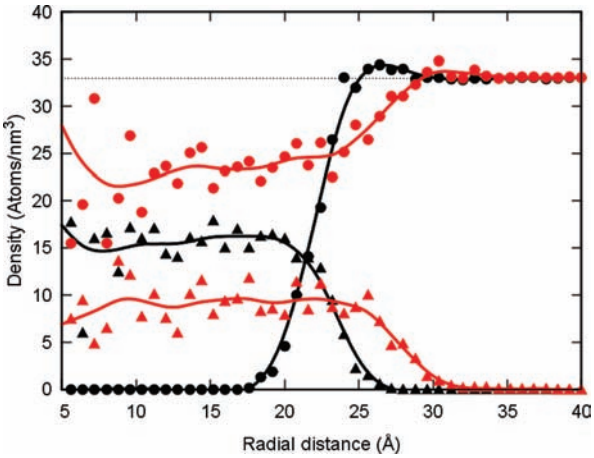

Figure 2. Density of calcium ions (▲) and water molecules (●) as a function of radius for the largest 864-atom ACC nanoparticle. Here the black and red lines correspond to anhydrous ACC and ACC with approximately 3 waters per formula unit, respectively. The dashed horizontal gray line indicates the experimental bulk density of water.

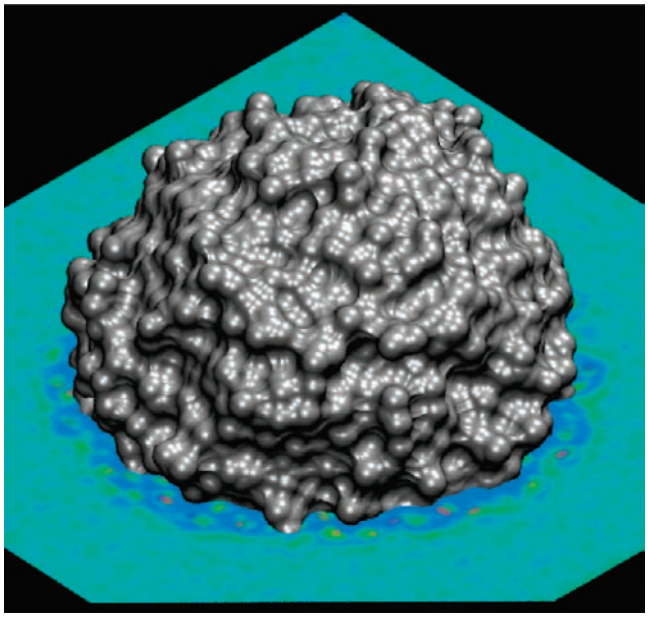

Figure 3. Ordering of water around a nanoparticle of amorphous calcium carbonate. The gray surface indicates a snapshot of the rough boundary of the solid, while the intersecting plane is color coded according to the oxygen density of water. Blue indicates regions of reduced water density, while green → red indicates increasingly localized and therefore structured water. To compare against calcite (10$\bar{1}$4), see Figure 8 of Raiteri *et al.*[23]

In comparing the size of the anhydrous and strongly hydrated ACC nanoparticles there is a significant difference in radius, as would be expected from the incorporation of water into the structure. Taking the radius to be the point at which the calcium ion density has decayed to half the average value within the nanoparticle, the radii of the anhydrous and hydrous ACC particles are 4.4 and 5.5 nm, respectively. Based on these values, the volume of water in ACC for the hydrated particle is 49.2 Å^3 per formula unit. The volume of a water molecule in monohydrocalcite computed with the present force field is 14.86 Å^3, which leads to an estimated stoichiometry of $CaCO_3 \cdot (3.3)H_2O$, consistent with the value of $CaCO_3 \cdot (3.1)H_2O$ obtained directly.

Before analyzing the properties of the ACC materials synthesized in the present work, it is important to examine the

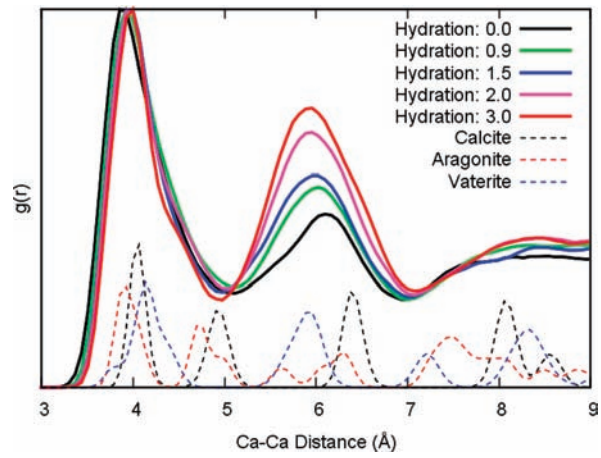

Figure 4. Radial distribution function (RDF) of Ca−Ca distances for an amorphous calcium carbonate nanoparticle containing 864 formula units as a function of $H_2O/CaCO_3$ ratio. The equivalent RDFs for bulk calcite, aragonite, and vaterite are given (using the ordered Wang and Becker model for vaterite), indicated by the black, red, and blue lines, respectively, in the lower portion of the plot. Note that the absolute magnitude of the RDF has been scaled down for the crystalline phases for clarity.

structure to ensure that it possesses the correct characteristics in relation to experimental data. Given the amorphous nature, much of the information available regarding the atomic structure of ACC comes from Ca EXAFS.[50,51] Literature results for the coordination number of Ca are somewhat dispersed, while the Ca−O distance also exhibits some variability.[52] The recent study of Michel *et al.*[10] obtains values of 6.7 and 6.1 (±25%) from fits to the results for two different synthetic samples, along with a Ca−O bond length of 2.41 Å. Our data for ACC agrees with this Ca−O distance and gives coordination numbers that are also close to those found experimentally for the same cutoff distance.

Pair distribution function (PDF) analysis has also been applied to ACC and has the benefit of offering insights into the medium range order within this material, leading to two significant peaks at ∼4 and 6 Å. Goodwin *et al.*[12] have utilized Reverse Monte Carlo (RMC) to create representative structures for ACC that are consistent with the PDF data. In this manner, it is possible to extract pairwise radial distribution functions for all species. Of these, the two curves that exhibit the greatest degree of structure are for the Ca−O and Ca−Ca pairs. Since the local structure for the Ca−O case has already been validated, we present our calculated results for the Ca−Ca distribution in Figure 4 as a function of hydration level. The overall structures of all of the Ca−Ca distributions match those of Goodwin *et al*. in containing two main peaks at the expected distances. Even more subtle features, such as the shoulder on the high distance side of the 4 Å peak seen in the experiment, are reproduced. The third broader peak in our results is at, or beyond, the limit of the data given by Goodwin *et al*. Furthermore, because our analysis is based on nanoparticles, rather than bulk material, the information at large distances becomes less certain since the presence of the surface begins to contribute to the RDF and therefore we do not consider this feature further.

(50) Taylor, M. G.; Simkiss, K.; Greaves, G. N.; Okazaki, M.; Mann, S. *Proc. R. Soc. London, Ser. B* **1993**, *252*, 75–80.
(51) Levi-Kalisman, Y.; Raz, S.; Weiner, S.; Addadi, L.; Sagi, I. *Adv. Funct. Mater.* **2002**, *12*, 43–48.
(52) Gunther, C.; Becker, A.; Wolf, G.; Epple, M. *Z. Anorg. Allg. Chem.* **2005**, *631*, 2830–2835.

Although the overall shapes and positions of the peaks in the Ca−Ca RDFs are not influenced by the degree of hydration, the ratio of the first to second peak heights is found to be strongly correlated with the presence of water, such that this can be used as a quantitative indicator. The RMC curve is found to closely match those from the simulated ACC nanoparticle when the water content is between 1 and 1.5 molecules per formula unit; a result that is also true for the pairwise distribution functions of other species. Despite the fact that this may appear to be slightly higher than the stoichiometric $CaCO_3 \cdot H_2O$ formula used in the RMC model, we note that the total scattering data were taken from the earlier work of Michel *et al*. in which the samples were characterized as containing water ratios of 1.38 and 1.19. Thus the identification of the hydration state based on the Ca−Ca RDF peak ratio appears to be consistent with what is known regarding the experimental materials.

Before leaving the subject of the structure, comparison should be made to the RDFs of the crystalline phases. As found in the previous PDF studies,[10] the structure of the present ACC material does not resemble that of any ordered phase, including the hydrated forms of calcium carbonate. While vaterite also has two peaks at ∼4 and 6 Å in the Ca−Ca profile, and has the closest overall resemblance, there are other characteristics that do not match for this phase. It should be noted that the experimental label ACC covers a variety of materials that sometimes includes phases that are described as having calcitic or vateritic short-range order.[53] Here we focus on ACC that is truly amorphous but recognize that there may be samples of ACC that have begun to develop local structural order within domains as they age.

Having characterized the structural properties of the ACC nanoparticles, we now turn to contemplate the thermodynamics of this system. In Figure 5a we show the calculated enthalpy for the particles as a function of increasing size from 18 to 864 formula units. While the free energy is the pivotal thermodynamic quantity, the accurate determination of the absolute magnitude of this quantity for a disordered material in contact with solution is a difficult undertaking for current computational methods. Consequently, we first consider the enthalpy, which is more readily obtained and offers insights in the low temperature limit, and then later return to examine the question of the free energy.

In addition to ACC, results are also given for nanoparticles of calcite with exclusively $(10\bar{1}4)$ facets. Based on observations of other materials, it is known that changes in the relative stability of different polymorphs can occur in the regime of nanoparticles,[6] and therefore it is important to consider whether the choice of calcite as a reference for crystalline calcium carbonate at this scale is appropriate. To test this we have also performed a limited number of simulations using the rigid variant of the present force field in which the ordered Wang and Becker structure of vaterite was used to generate crystalline nanoparticles. Despite the very different structure and particle morphologies, the enthalpies of the vaterite nanoparticles were found to track those of calcite on the energetic scale being considered here, as might be expected from the bulk energy difference. Given that this phase represents the most extreme difference possible within the crystalline phases, based on bulk energetics, it is anticipated that aragonite nanoparticles would also be barely distinguishable on the scale of the enthalpy

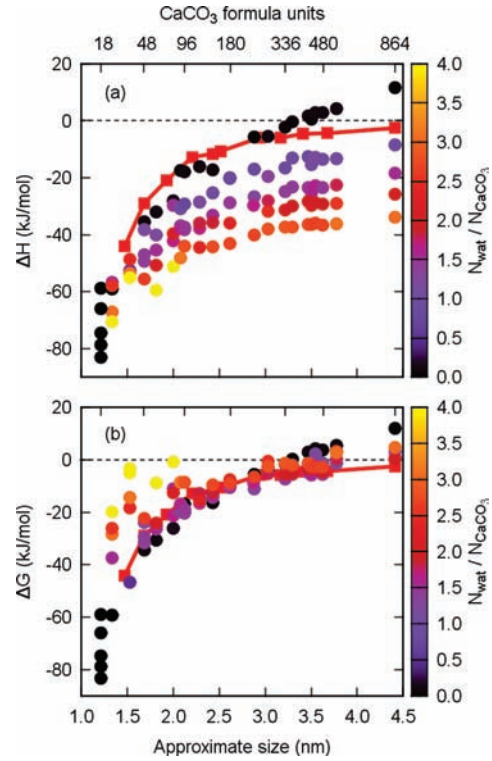

Figure 5. Enthalpy (a) and free energy (b) per formula unit as a function of $CaCO_3$ cluster size. Here circles and squares represent data points for amorphous calcium carbonate and calcite, respectively. Circles are color coded according to the water content per formula unit, while points for calcite are in red.

differences between ACC and calcite. Although no definite conclusions can be drawn in the present work, since the comparison of crystalline nanoparticles was not the objective, there appears to be no enthalpic stability crossover between calcite and vaterite in the cases considered.

The dominant trend with increasing particle size for all forms of calcium carbonate is that of an increasing enthalpy per formula unit. This is to be expected based on the fact that the dissolution enthalpy for calcite is exothermic, and so a smaller surface to volume ratio leads to an increased enthalpy per formula unit due to the reduced contact with water. It is important to note that with other force field models where the dissolution enthalpy is positive this would not be the case, thereby emphasizing the importance of having the correct sign for this quantity. In the case of the calcite nanoparticles, the enthalpy is correctly asymptotic to the internal energy of the bulk phase for the present model corrected by the contribution from the phonons, as given by the equipartition theorem.

The second trend that is apparent is that the enthalpy of ACC clusters/nanoparticles decreases as the incorporation of water into the structure increases. Again, this is consistent with an exothermic enthalpy of dissolution. For the largest nanoparticle considered, the total stabilization of the most strongly hydrated form of ACC relative to the anhydrous material actually exceeds the dissolution enthalpy. This occurs because the first waters of solvation for a calcium cation generate a more exothermic contribution than the latter ones as the coordination number increases.[54] It is important to note that there is a clear and consistent trend in regard to the decreasing enthalpy with

(53) Gebauer, D.; Verch, A.; Borner, H. G.; Colfen, H. *Cryst. Growth Des.* **2009**, *9*, 2398–2403.

(54) Bako, I.; Hutter, J.; Palinkas, G. *J. Chem. Phys.* **2002**, *117*, 9838–9843.

increasing hydration across the range of particle sizes. Given that the generation of each particle size is performed independently, there is no correlation between data points. Hence, the existence of a definite trend strongly suggests that the results are statistically significant since all simulations are achieving a distribution of states with similar characteristics, regardless of their different histories.

Comparing the relative enthalpies of calcite and ACC as a function of particle size, there is an apparent crossover in stability. For small clusters (containing less than 200−300 formula units), all forms of ACC, including the anhydrous one, have a lower enthalpy than calcite. Above particle sizes of ∼300 formula units, anhydrous ACC possesses a higher enthalpy than calcite and increases in enthalpy more rapidly with size than its crystalline competitor. For a water content of 0.5−1.0 per formula unit, the enthalpy of ACC remains lower than calcite up to the maximum size of prenucleation clusters observed experimentally, though the enthalpy difference is decreasing as the particles grow. Although there is no experimental data to directly compare against, the current results are consistent with observations that the stability of ACC is variable and that this correlates with water content. Experimentally it has been proposed that "transient" ACC is largely anhydrous, while "stable" ACC contains water to an extent in the region of one molecule per formula unit.

While the amorphous nanoparticles show a trend of increasingly negative enthalpies as the water content increases, it is important to consider the entropic contribution that will counter balance this. At present, it is a challenging, and arguably intractable, problem to determine the entropies of hydration for amorphous nanoparticles containing large quantities of water. However, there is a considerable amount of data in the literature concerning the entropy change associated with the incorporation of water into solids. Indeed, it is found that this quantity is remarkably constant within a given family of compounds, and even across different materials. For example, Mercury *et al.*[55] quote average entropies for water in hydrated materials of 41.5, 42.5, 43.7, and 45.8 J K^{-1} mol^{-1} for sulfates/sulfites, hydroxides/oxyhydroxides, chlorides/chlorates, and ices, respectively. The largest standard deviation is ±17.1 J K^{-1} mol^{-1} for hydroxides and oxyhydroxides, which is unsurprising since water is chemically dissociated in these materials. The other classes show reduced standard deviations of ±6 J K^{-1} mol^{-1} or less.

In the case of carbonates, experimental data are also available regarding the entropy for water incorporation relative to bulk liquid.[56] There are two crystalline hydrates of calcium carbonate, monohydrocalcite ($CaCO_3 \cdot H_2O$), and ikaite ($CaCO_3 \cdot 6H_2O$). Both of these phases have a negative enthalpy of formation with respect to calcite but are unstable with respect to the same phase at ambient conditions based on the free energy. Using the experimental data, the entropy change per water is 32.0 and 33.5 J K^{-1} mol^{-1} for monohydrocalcite and ikaite, respectively. This again demonstrates the remarkable consistency for values, regardless of the total water content and nature of the structure. Even for the magnesium carbonate of landsfordite ($MgCO_3 \cdot 5H_2O$), a similar value of 33.1 J K^{-1} mol^{-1} is obtained. Based on this consistency, we propose that the relative free energy of different hydration states of ACC can be determined by applying a constant correction per water molecule to allow for the entropy of water incorporation.

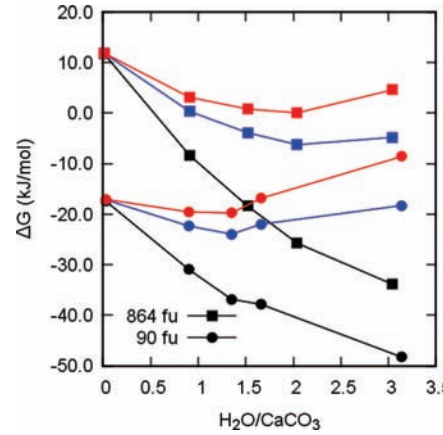

Figure 6. Energies per formula unit as a function of water content for two different sizes of ACC nanoparticle at the extremes of the size distribution. Here black symbols represent the enthalpy, while the red and blue symbols indicate the free energy based on the correction for the entropy of water incorporation at 298.15 K using the theoretical and experimental estimates, respectively. Lines are provided only as a guide to the eye and adopt the same color code as the symbols.

Converting the entropy change per water molecule at 300 K to a free energy contribution ($-T\Delta S$) yields values of +9.59 and +10.04 kJ/mol for monohydrocalcite and ikaite, respectively. While one approach would be to employ the experimentally determined quantities as a correction, here we also compute the same value based on the actual model used in the simulations in order to be consistent. Here only the difference between calcite and monohydrocalcite is considered, since the latter phase is closer to the relevant composition range than ikaite. For the solid phases, the entropy difference is computed based on the phonon density of states, integrated across the Brillouin zone with a sufficiently fine Monkhorst−Pack mesh so as to achieve convergence. The gas phase entropy of a water molecule was explicitly calculated since this deviates from the experimental value as the optimized geometry of SPC/Fw water leads to small differences in the principal components of the moment of inertia tensor. For the present model, the computed free energy contribution associated with water incorporation is found to be +12.68 kJ mol^{-1}, which corresponds to an entropy difference of 42.3 J K^{-1} mol^{-1}. Although higher than the experimentally measured value for monohydrocalcite, the calculated entropy change is physically reasonable, being very similar to values previously reported for other classes of material.

The comparison of the enthalpies and relative free energies, as computed by application of the above entropy correction, is illustrated in Figure 6 for two ACC clusters at the extremes of the size distribution. It is readily apparent that this entropic correction has a significant influence on the stability trends. While the enthalpy systematically decreases as a function of increasing water content, the free energy for both particle sizes passes through a minimum and ultimately increases as further water is added.

By locating the favored hydration state for each cluster size, this quantity can be plotted as a function of approximate radius (Figure 7). Although there are fluctuations as a result of the variations between particles of different sizes, there is a clear trend toward increasing hydration with increasing radius. For a cluster containing 90 formula units, the optimal $H_2O/CaCO_3$ ratio is in the region of 1−1.4, while for the other extreme of

(55) Mercury, L.; Vieillard, P.; Tardy, Y. *Appl. Geochem.* **2001**, *16*, 161–181.
(56) Konigsberger, E.; Konigsberger, L. C.; Gamsjager, H. *Geochim. Cosmochim. Acta* **1999**, *63*, 3105–3119.

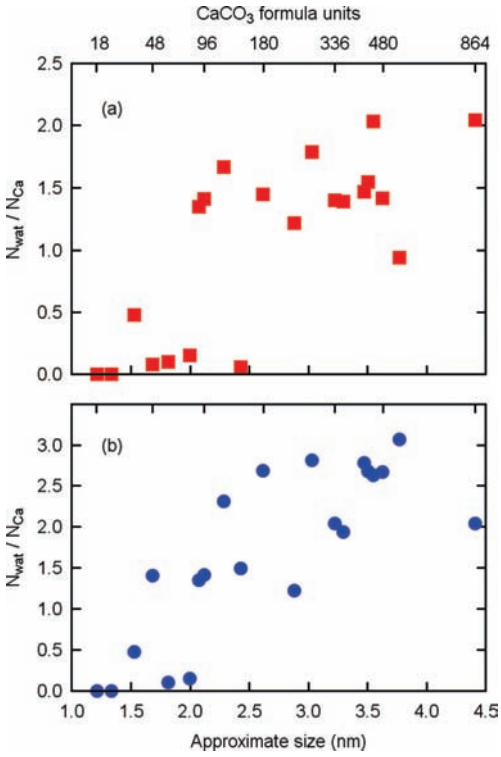

Figure 7. Variation of the thermodynamically favored water content per formula unit of calcium carbonate in ACC as a function of cluster size. Values that minimize the free energy are plotted based on the theoretical (red) and experimental (blue) entropy corrections in the upper and lower panels, respectively.

the largest nanoparticle considered this value has increased to ~2. The other particles lie at intermediate values, as expected. These predicted water contents are slightly higher than those expected from experiment, a point we will return to below. Varying the entropy correction between that found experimentally and that computed leads to no qualitative change in the results, demonstrating that the trend is robust with respect to the quantitative details. The key finding is that the thermodynamically favored degree of water incorporation into amorphous calcium carbonate will *increase* as the size of the cluster or nanoparticle *increases*.

Previous computer simulations[22] have proposed that water is incorporated into amorphous calcium carbonate as a consequence of kinetics; in other words the water is trapped because it cannot escape due to the speed of growth. While our results so far say nothing about the kinetics, it is demonstrated that there is no requirement to invoke a kinetic argument to justify the presence of water in ACC since this is the thermodynamically preferred state for larger particles. Indeed, the previous simulations employed a model that has a large positive enthalpy of dissolution and a high degree of supersaturation, all of which may have overemphasized kinetic effects due to the enhanced rate of agglomeration.

Where kinetics may play a role is in the evolution of the nanoparticles. For small clusters, it should be feasible for the system to achieve the equilibrium structure with respect to water incorporation due to the high surface to volume ratio, resulting in labile solvent exchange. As the cluster grows, it will become harder for the core of the particle to reach equilibrium with the surrounding solution if a point is reached where the diffusion rate of water in hydrous ACC is slower than the rate of growth. Experimentally, it is known that water interconversion in ACC is hindered and processes have been measured to occur on the millisecond time scale.[10] Hence, depending on the degree of supersaturation, growth may well occur faster than the diffusion of structural water. When this is the situation, it implies that the water content of ACC nanoparticles will in fact be heterogeneous; the core will have a lower degree of hydration than the outer shell. Consequently, the $H_2O/CaCO_3$ ratio for larger particle sizes, as predicted based on the free energy minima, will represent an upper bound to the actual water content when kinetic factors are important. This may contribute to the apparent overestimation of the level of water incorporation in the present work relative to experiment for larger nanoparticles.

In addition to considering the hydration state of ACC clusters, it is important to examine the stability relative to calcite nanoparticles in light of the entropic correction. Here it is assumed that the differential contribution of the phonon entropy is negligible and therefore the internal energy of calcite can be taken as the free energy, while recognizing that both this phase and ACC may undergo a similar constant offset to the absolute free energy. In the case of bulk calcite it has already been shown that the difference between the free energy and enthalpy at 298.15 K is less than 0.5 kJ/mol in the present model and so the difference between this value and the same quantity for ACC is likely to be an order of magnitude smaller again. Figure 5b shows the relative free energies for both ACC and calcite as a function of particle size. Below a diameter of ~3.8 nm ACC in its favored hydration state is always more stable than calcite for the same number of formula units. Above this critical size the free energy of ACC continues to increase while that of calcite has almost reached the plateau associated with the bulk value, leading to a reversal in the stability. Interestingly, this diameter is similar to that of the largest prenucleation cluster observed by Gebauer *et al*. However, this may be coincidental given that there is no reason why the ACC nanoparticles cannot continue to grow while being metastable. Only if competition for growth between calcite and ACC exists in the same system would the ACC particle size be expected to stop at this dimension.

So far it has been necessary to approximate the free energy of the calcium carbonate systems based on predefined states. In order to offer further confirmation of the stability of ACC clusters, and to provide greater insight into the growth processes, an alternative approach to determining relative free energies is considered. While it remains challenging to accurately determine the absolute free energy of any given cluster, the relative free energy can be examined incrementally. To do this we consider the process whereby an additional calcium carbonate formula unit is added to an existing cluster. Provided a good choice of the reaction coordinate exists, the free energy profile can be reliably determined for this process. Here we consider the growth process to occur via addition of a contact Ca^{2+}/CO_3^{2-} ion pair, as illustrated in Figure 8, using the minimum distance between the calcium and carbon atoms of the ion pair and of the cluster for the collective variable, as proposed by Tribello *et al*.[22] The choice of the ion pair as the growth unit will be justified later in the context of the results below. However, even if the ions add individually, or via a solvent separated ion pair, the free energy for the final states (particle with $n+1$ formula units) will remain unchanged, while the initial state (particle with n formula units) will be shifted by a constant offset for all particle sizes.

Before considering the results for the free energy profiles it is important to describe the point of reference for the zero of

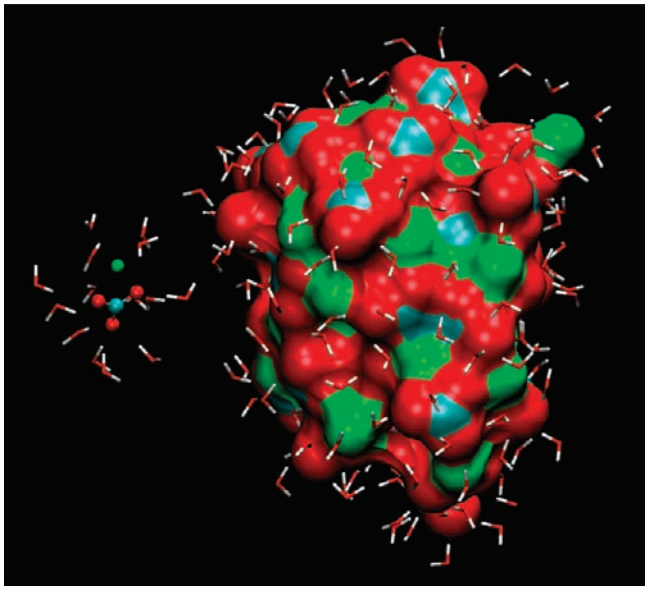

Figure 8. Illustration of a $CaCO_3$ ion pair being added to an ACC cluster. Here calcium, carbon, oxygen, and hydrogen are colored green, blue, red, and white, respectively. Only the first solvation shell of each species is explicitly shown.

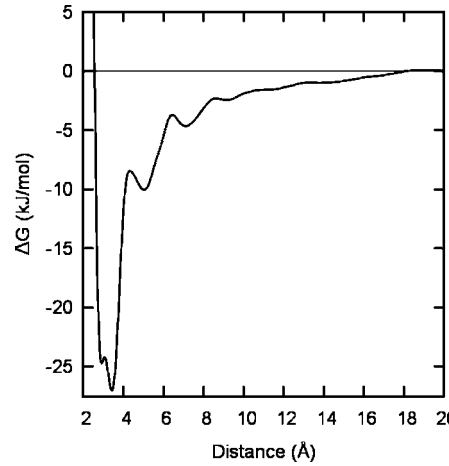

Figure 9. Free energy profile for ion-pair formation from a calcium and carbonate ion in aqueous solution as a function of distance between the calcium and carbon atoms. The free energy is defined relative to the configurational entropy contribution as described in the text.

the energy scale. If the removal of an ion pair from a cluster is considered (i.e., the dissolution, rather than growth process) then the internal energy of interaction will ultimately decay to the energy of the fragments at infinite separation in water. If we now consider the free energy, then the situation is more complex. While most of the contributions to the free energy also become asymptotic to that of the infinitely separated fragments, there is a configurational entropy term that follows a different limiting form. For two particles constrained to be a distance r apart from each other, then the number of available degenerate microstates increases in proportion to $4\pi r^2\,dr$ (i.e., the surface area of the sphere defined by one particle moving around the other). Hence, the free energy difference to move between two separation distances, $r_1 \rightarrow r_2$, involves a contribution of $k_BT\ln(r_1^2/r_2^2)$ arising from the configurational entropy. In all of the values reported here this limiting contribution has been subtracted by fitting the decay of the free energy in the long-range limit, such that this quantity becomes asymptotic to the sum of the contributions for the separated fragments. Because one of the fragments is actually a particle of finite size, it is necessary to add the effective radius of the cluster to the reaction coordinate in order to obtain the correct radial distance for the entropy correction.

At first the above configurational entropy correction may appear to be a technical curiosity. However, it is physically very important since this provides a concentration dependence of the free energies. Concentration controls the mean distance between the separated growth units, representing r_1, while the bound state determines the final r_2. Therefore the configurational entropy correction provides a distance dependent positive shift to the baseline of the free energy that determines the thermodynamic driving force for growth/dissolution as a function of concentration.

The free energy profile for forming a calcium carbonate contact ion pair is shown in Figure 9. The deepest minimum, in the region of 3 Å, is actually split into two configurations with a slight barrier between them. The inner state corresponds to a bidentate binding of carbonate to calcium, while the more stable configuration at longer distance is the monodentate form. In addition, there are two further distinct minima due to solvent separated ion pairs with one or two intervening water molecules. Beyond this the free energy landscape is only weakly structured with no barriers approaching thermal energy at ambient conditions. The free energy of ion pairing is found to be −27 kJ/mol. In the previous work of Tribello *et al*. the free energy of the monodentate ion pair was found to be very similar.[22] However, this configuration was only a point of inflection in the free energy leading to a bidentate arrangement that was more stable by 8 kJ/mol. At least within the structure of ACC there is experimental evidence that a monodentate binding of carbonate to calcium ions is preferred.[10] Using the experimental equilibrium constant for the ion pair of Plummer and Busenberg,[48] the standard free energy is computed to be −18.4 kJ/mol. In comparing our calculated value to experiment it is necessary to correct for the concentration dependence. By taking the mean distance between completely dissociated ion pairs in a 1 M solution of calcium carbonate, the concentration correction can be estimated to be +5 kJ/mol, leading to a standard free energy for ion pairs of −22 kJ/mol. Although the present value is slightly more exothermic than many of the experiment estimates, it does lie within the distribution of measured values.[48]

Having demonstrated that $CaCO_3$ ion pairs represent an appropriate reference point on the free energy landscape, as they possess a lower free energy than the separated ions at standard conditions, it is now possible to consider the addition of these growth units to other systems. First, we should consider the situation with respect to growth of the basal plane of calcite as a point of reference. Considering the ions alone, neither calcium cations nor carbonate anions exhibit favorable binding directly to the solvated $(10\bar{1}4)$ surface of calcite.[23] With the present model there is no thermally accessible minimum corresponding to calcium binding at the surface, either solvent separated or directly. Although carbonate exhibits two minima above this surface, it only binds weakly in states where it is solvent separated. In light of this, it is not surprising to discover that a charge neutral ion pair possesses a similarly weak interaction with the $(10\bar{1}4)$ surface forming only a solvent separated state at ∼5 Å above the first layer of calcium carbonate, with a free energy of binding of 7 kJ/mol. From these results, it is obvious that growth will not occur on the pristine $(10\bar{1}4)$ surface of calcite, in accord with experimental observations that the growth of calcite is usually nucleation limited and relies on the presence of kink sites, such as those at surface edges, pits, and

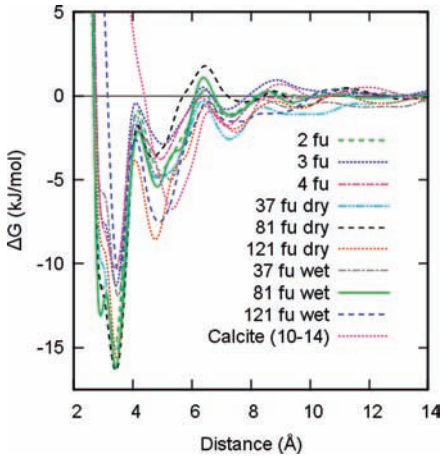

Figure 10. Free energy profile for addition of a $CaCO_3$ ion pair to clusters of nominally anhydrous amorphous calcium carbonate. Here the label of $(n + 1)$ fu refers to the free energy profile for a final state in which a cluster containing this number of formula units is formed (i.e., the binding of an extra ion pair to n formula units). The equivalent free energy profile for addition to the $(10\bar{1}4)$ surface of calcite is also shown for comparison. For the clusters, the free energy is defined relative to the configurational entropy contribution, as described in the text, while for the calcite surface no correction is required.

screw dislocations.[57] Translating this to calcite nanoparticles, where water also exhibits the structural ordering characteristic of the basal plane,[58] we find that growth on the exposed surfaces is unfavorable and so addition of ion pairs is limited to the edges of the crystallite. Because ions do not associate with or diffuse across the $(10\bar{1}4)$ surface, this growth requires direct diffusion through aqueous solution leading to collision with the edge, resulting in a low prefactor for growth. In contrast, the ACC particles have a rough, approximately spherical, morphology and ion pairs can add by collision with any part of this surface, thus giving rise to a much higher prefactor than that for crystalline nanoparticles.

Turning now to contemplate the free energy profile for ion pair binding to amorphous calcium carbonate clusters, the results are shown in Figure 10 for a range of sizes from the ion pair dimer through to the addition to a particle with 120 formula units. Here simulations are performed for both the nominally anhydrous ACC and clusters containing approximately 1.5 water molecules per formula unit. However, for the smaller cluster sizes the definition of a particular hydration state has no physical meaning since they represent the initial stages of agglomeration of ion pairs in water. The first striking feature of the free energy profiles is their similarity over a widely varying cluster size, all the way from the ion pair dimer to the largest particle of ACC considered. In all cases the addition of an ion pair is found to be exothermic with a binding energy of between 10 and 16 kJ/mol. There appears to be no systematic change in this binding energy as a function of increasing size. Even the influence of water content fails to significantly change the profile. Although we have not performed the systematic addition of every single ion pair over the whole range of composition, sufficient states have been sampled to suggest that this relatively constant value for the free energy of binding would be found for all ion pairs up to the largest size examined.

Two minima are actually found in the distance range of 2.5−4 Å at which the ion pair becomes part of the cluster. Although this is reminiscent of the bidentate vs monodentate structures of a single ion pair, the cause is different. As demonstrated by Tribello *et al*.,[22] the inner, less stable, configuration corresponds to two carbonate anions bridging the same two calcium ions, while the outer of the two minima represents carbonate groups both bridging between different cations. As the cluster size increases, the presence of the inner minimum becomes less pronounced and approaches being a point of inflection. Aside from the minima in which the ion pair has become part of the cluster, there are two distinct solvent separated states observed. During the transition from small groups of ion pairs to genuine ACC particles, these minima become deeper, approaching a binding energy of 8 kJ/mol for the single layer of solvent separating the fragments. In order to migrate between the three overall minima on the potential energy surface, the system has to pass through a point close to the zero of the free energy scale in each case. Hence, the activation free energy for growth would correspond to the well depth for the solvent separated state, plus any contribution from the concentration correction. Since this represents only six times the ambient thermal energy per degree of freedom at room temperature, the growth process is only weakly activated and is more likely to be diffusion limited.

The present results validate the findings of Gebauer *et al*.[5] and demonstrate that the prenucleation clusters are indeed stable, rather than metastable as would be the expectation from classical nucleation theory. Indeed, we can also examine some of the assumptions made in the data analysis by Gebauer *et al*. In their work, it was assumed that the equilibrium constants for successive additions of either Ca^{2+} or CO_3^{2-} to clusters of varying size were all equal (see Figure S7 in their Supporting Information). At first sight this might appear to be a drastic approximation. However, it has been shown here that the free energy of binding of an ion pair to ACC prenucleation clusters is indeed largely independent of size and, to a lesser degree, composition. It is also possible to make a quantitative connection with this experimental data. In our scheme, there are two distinct reaction steps: formation of an ion pair and binding of this ion pair to the cluster. Therefore if we make the same assumption as Gebauer *et al*., i.e. that there is a single uniform growth step with one equilibrium constant, then we must take the average of the free energy changes for our two-step process. Taking the midpoint of the energy range for ion pair binding, we arrive at a free energy for formation of an ion pair in a cluster of −20 kJ/mol, in good agreement with the value of −18.5 kJ/mol (at pH 8.5) from Gebauer *et al*.

The combination of the two above approaches to determining the free energy of amorphous calcium carbonate has demonstrated that the small clusters are both stable with respect to ions in solution, under an appropriate degree of supersaturation, and also relative to nanoparticles of calcite below a size of ∼4 nm. In addition to the thermodynamic information, we can predict that the initial growth of ACC prenucleation clusters will be fast, given that the activation barrier is only a small multiple of ambient thermal energy and that the effective collision prefactor will be higher than that for crystalline phases.

Conclusions

Through the use of accurate force field simulations we have provided detailed thermodynamic data at the atomistic level that supports the experimental results of Gebauer *et al*. while providing further new insights into the growth of ACC. While Meldrum and Sear[7] speculate that the presence of impurities may be necessary to stabilize precritical clusters of ACC, our study suggests that they are already stable while pure and thus it is unnecessary to invoke the presence of impurities. Furthermore, we find that the free energy profile for addition of ion pairs of calcium carbonate to ACC

(57) Gratz, A. J.; Hillner, P. E.; Hansma, P. K. *Geochim. Cosmochim. Acta* **1993**, *57*, 491–495.
(58) Cooke, D. J.; Elliott, J. A. *J. Chem. Phys.* **2007**, *127*, 104706.

nanoparticles remains remarkably constant as a function of particle size. While ACC and the calcite $(10\bar{1}4)$ surface, which dominates the morphology of this material, both have a free energy minimum for an ion pair separated by one solvent layer from the particle, only for the ACC particles is surface addition favorable, thus explaining why the amorphous phase is able to grow rapidly in comparison to other ordered phases. This occurs as a result of the ACC−water interface constantly being rough and in a state of flux, therefore lowering the barrier to crossing the aqueous interface, which is highly structured for crystalline surfaces.[49] The rate of water exchange in coordination complexes is known to be an important factor and often the key to reactivity. It has been demonstrated that rate constants for such processes can be reliably calculated using the reactive flux approach for a variety of aluminum species in aqueous solution and at interfaces.[59] Such an approach could also be applied to the present system in future work.

Incorporation of water into the amorphous calcium carbonate nanoparticles is found to be driven by thermodynamic stability. Although kinetic factors may be important during rapid growth, leading to water being trapped as postulated elsewhere,[22] this is not required to explain the hydration state since water will be incorporated at equilibrium. Although the enthalpy decreases monotonically as the level of water increases in the ACC particles, when the entropic penalty for removal of water from the bulk is corrected for a minimum in the free energy occurs. The favored stoichiometry of ACC is found to be dependent on the size of the particle; as the size of the particles increases so does the water content per formula unit of calcium carbonate. Under conditions where clusters are growing very rapidly, this implies that the core of the ACC particle may be drier than the outer regions, at least until the water can diffuse and reequilibrate. This inhomogeneity in the distribution of water may well explain the nature of the recent structure proposed for bulk amorphous calcium carbonate determined by Reverse Monte Carlo analysis of experimental pair distribution function data. Here Goodwin *et al.* find representative structures that resemble a disordered framework material in which there are channels that are water rich, separating regions of amorphous calcium carbonate with reduced water content. Based on our model, such a structure would arise if nanoparticles with a drier core and wetter shell agglomerate during the second phase of growth, as proposed by Pouget *et al.*,[8] but the rate of water diffusion is slow, such that a homogeneous distribution cannot be attained.

In terms of the overall formation of calcium carbonate from homogeneous solution, all of the evidence presented here supports the adoption of a nonclassical mechanism for nucleation and growth. Stable clusters of ACC can be formed with an activation barrier comparable to ambient thermal energy by using the combination of a rough surface to disrupt the surrounding water structure and the incorporation of increasing levels of water with expanding size to lower the free energy. Although such clusters ultimately become metastable with respect to crystalline nanoparticles of calcite (and the other polymorphs of calcium carbonate), their free energy can always remain lower than the ions in solution, avoiding the need for metastable nuclei. While Gebauer *et al.* refer to these stable species as prenucleation clusters, we propose that this is actually the nucleation step and that growth of amorphous calcium carbonate is not nucleation limited. A schematic representation of this pathway is given in Figure 11. As the nanoparticles increase in size, the driving force for growth will decrease; the free energy for addition of an ion pair is more exothermic for a small cluster than for a larger one. This is consistent with the experimental observation of the preferential formation of a narrow distribution of smaller clusters during the early stages of growth. These particles can subsequently agglomerate by diffusion.

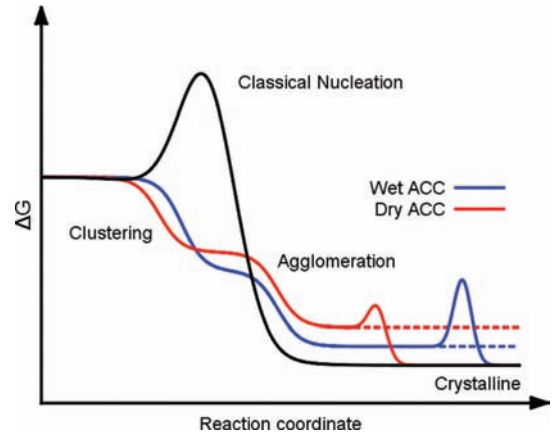

Figure 11. Schematic representation of the free energy profile for the nonclassical formation of calcium carbonate from ion pairs in solution. Here the two lines for ACC represent the bounds of a distribution of possible curves depending on the water content. The final transformation of ACC to a crystalline polymorph can occur at variable reaction coordinate depending on the environmental conditions.

The barrier to formation of ordered $CaCO_3$ arises due to the transformation of either individual or agglomerated metastable ACC nanoparticles beyond the critical size of ∼4 nm into (poly)crystalline material. This event can be triggered by a number of environmental conditions, including contact with proteins, self-assembled monolayers, or any other factor that will promote the nucleation of an ordered region within the amorphous phase.[60,61] This order−disorder transformation may well represent a classical nucleation process after all, but during the second stage of the growth process. Hence, while the nucleation and growth of amorphous calcium carbonate is nonclassical, the conversion of this material to crystalline polymorphs may be classical instead. Future work will aim to seek the mechanism of what is considered to be an "enigmatic" transformation.[62]

Acknowledgment. The authors thank the Australian Research Council for funding through the Discovery Program as well as iVEC and NCI for the provision of computational resources. We also acknowledge valuable discussions with Franca Jones, David Quigley, Mark Rodger, and Gareth Tribello.

JA108508K

(59) Wang, J.; Rustad, J. R.; Casey, W. H. *Inorg. Chem.* **2007**, *46*, 2962–2964.

(60) Sommerdijk, N. A. J. M.; de With, G. *Chem. Rev.* **2008**, *108*, 4499–4550.

(61) Nudelman, F.; Sonmezler, E.; Bomans, P. H. H.; de With, G.; Sommerdijk, N. A. J. M. *Nanoscale* **2010**, *2*, 2436–2439.

(62) Politi, Y.; Metzler, R. A.; Abrecht, M.; Gilbert, B.; Wilt, F. H.; Sagi, I.; Addadi, L.; Weiner, S.; Gilbert, P. *Proc. Natl. Acad. Sci. U.S.A.* **2008**, *105*, 17362–17366.

(63) Wolf, G.; Konigsberger, E.; Schmidt, H. G.; Konigsberger, L. C.; Gamsjager, H. *J. Therm. Anal. Calorim.* **2000**, *60*, 463–472.

(64) Markgraf, S. A.; Reeder, R. J. *Am. Mineral.* **1985**, *70*, 590–600.

(65) Redfern, S. A. T.; Angel, R. J. *Contrib. Miner. Petrol.* **1999**, *134*, 102–106.

(66) de Villiers, J. P. R. *Am. Mineral.* **1971**, *56*, 758.

(67) Effenberger, H. *Monatsh. Chem.* **1981**, *112*, 899–909.

(68) Megyes, T.; Grosz, T.; Radnai, T.; Bako, I.; Palinkas, G. *J. Phys. Chem. A* **2004**, *108*, 7261–7271.